

PRESENTED PAPER ON 4<sup>TH</sup> INTERNATIONAL  
RILEM-CONFERENCE ON  
*'REFLECTIVE CRACKING IN PAVEMENTS'*

Influence of a high modulus geogrid composite on the surface layer of  
roads on soft soil

J.M. Elias, Colbond Geosynthetics, the Netherlands  
A. Scarpas, Delft University of Technology, the Netherlands  
X. Liu, Delft University of Technology, the Netherlands

**Abstract**

In order to gain some insight about the mechanisms and the phenomena involved in the transfer of forces between a high modulus subbase reinforcement and the surrounding materials, a finite-elements system has been utilized. The influence of the reinforcement on the total paved road structure was assessed. Several issues were addressed like simulation of the bond characteristics of the reinforcement, simulations of the no-tension carrying characteristics of the aggregate materials, simulation of the propagation of discrete cracks in the pavement and their interaction with the surrounding materials. Practical design charts are presented for reinforced paved roads on soft subsoil.

**1. Introduction**

The use of geosynthetics as reinforcement in road construction has increased significantly over the past twenty years. Extensive use is now being made of a wide range of geosynthetics to improve road performance and or to economise in road construction. Geosynthetics can be placed in the asphalt and/or in the granular layers of a pavement in order to enhance the tension carrying characteristics of the material.

In order to gain some insight about the mechanisms and the phenomena involved in the transfer of forces between the reinforcement and the surrounding materials finite element analyses can be used [1]. The Delft University of Technology developed a finite elements (FEM) system, CAPA-2D [2], which has been utilized. A variety of options enable the quantification of the contribution of reinforcement in carrying tensile forces, the simulation of the no-tension carrying characteristics of the aggregate materials, the simulation of discrete cracks in the pavement and their interaction with the surrounding materials.

**2. Multifunctional geogrid composite**

In this FE-study a new geogrid composite has been used [3]. This geogrid composite has multifunctional properties by combining reinforcement, separation and filtration in one product. It is constructed from a coated high modulus aramid grid and a polyester nonwoven. The maximum strain is 3.5%. The geogrid composite has biaxial properties meaning that the strength is equal in both lengthwise and crosswise direction. This makes it suited for stabilization of soft, low bearing capacity soils and makes it possible to reduce

the base thickness of civil engineering structures, like temporary haul roads or permanent paved roads.

### 3. Fracture mechanics aspects of FEM crack simulation

Cracks introduce physical discontinuities in the otherwise homogeneous - for engineering analysis purposes - body of the pavement. Because their stiffness is usually low, if not zero, their presence plays a major role in determining the integrity and hence the load carrying capacity of the pavement.

The discontinuous nature of cracks renders inappropriate the application of classical continuum based layered analysis methods. On the other hand, by means of context of the FEM, cracks in the body of the pavement can be easily simulated by disconnecting the nodes of elements on either side of the crack propagation path, Fig. 1.

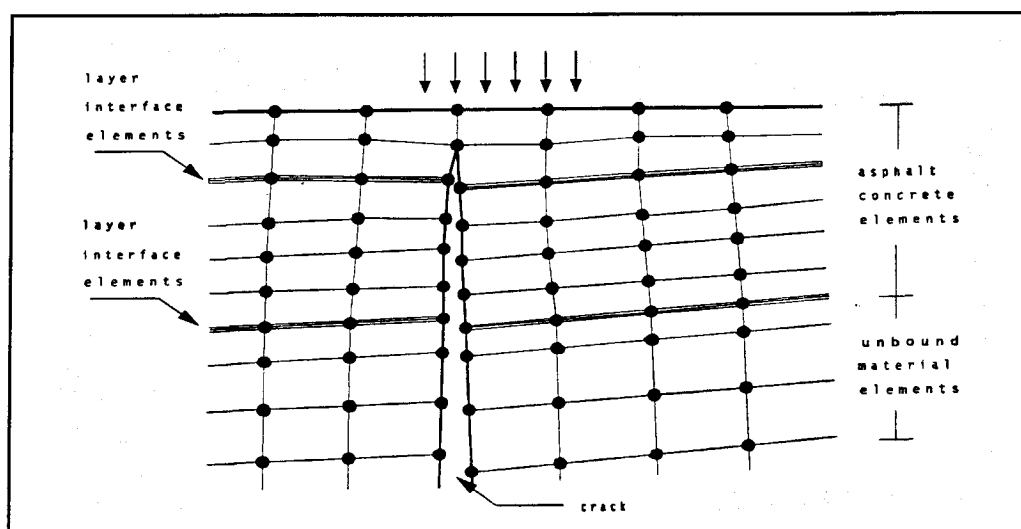


Figure 1 Finite elements crack simulation

Within the context of the FEM, the singularity of strains in the vicinity of a crack tip can be modelled accurately and elegantly if the elements surrounding the crack tip node are substituted by specially developed crack tip elements. Several special elements have been developed over the years.

### 4. Layer interfaces idealization

The successive material layers in a pavement structure are seldomly, if ever, rigidly bonded to each other. Depending on the nature of the materials and the construction techniques involved, some magnitude of interlayer slip can occur. The degree of interlayer bonding can influence significantly the overall structural response.

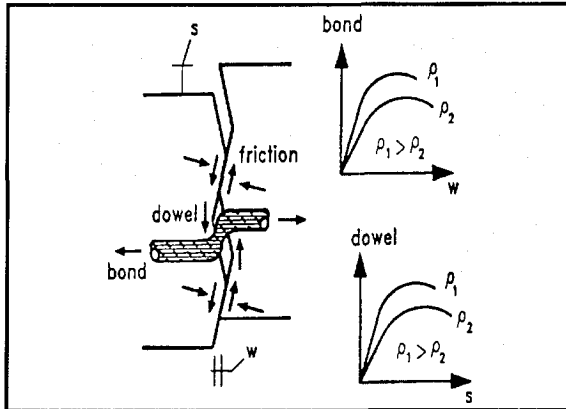


Figure 2 Relative displacements at an interface

The local response of the contact region between two interacting bodies of material can be described in terms of a relative displacement  $s$  and a relative, normal to the interface midplane, displacement  $w$ , Fig. 2. It is these two displacements that are meant to be modelled by means of an interface element. Only local behavior is simulated by a single element. The overall behavior can be simulated by a series of elements placed along the trace of the interface.

2-D interface elements were introduced to simulate the regions of physical discontinuity. The constitutive relation associating local stresses to relative local displacements is expressed as:

$$\begin{Bmatrix} \tau \\ \sigma \end{Bmatrix} = \begin{bmatrix} D_{tt} & 0 \\ 0 & D_{nn} \end{bmatrix} \begin{Bmatrix} s \\ w \end{Bmatrix} \quad (1)$$

in which  $D_{tt}$  is the shear stiffness of the interface and  $D_{nn}$  is the normal stiffness. By varying the shear stiffness terms, various types of bond can be specified. In general, these stiffness coefficients depend on both the state of stress and the deformation [4]. Determination of their values can be obtained by interface testing experiments.

### 5. FEM aspects of crack propagation simulation in pavements

A schematic representation of a typical finite elements simulation of a cracked pavement is shown in Fig. 3.

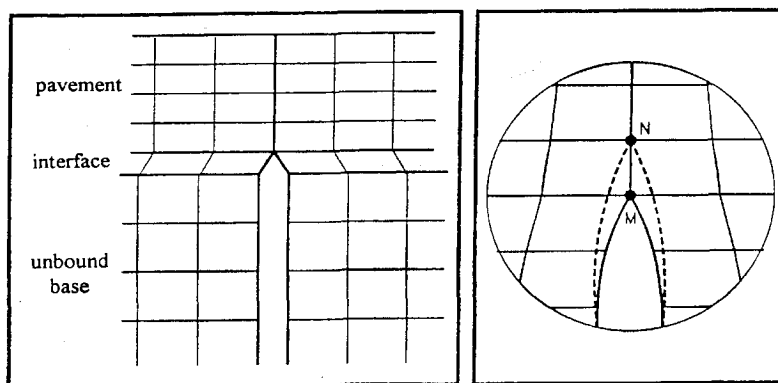


Figure 3 Schematic of FEM simulation of a cracked unbound base layer and crack propagation.

Since unbound base materials exhibit lack of tensile strength and stiffness, the original crack tip is normally placed at the bottom of the pavement.

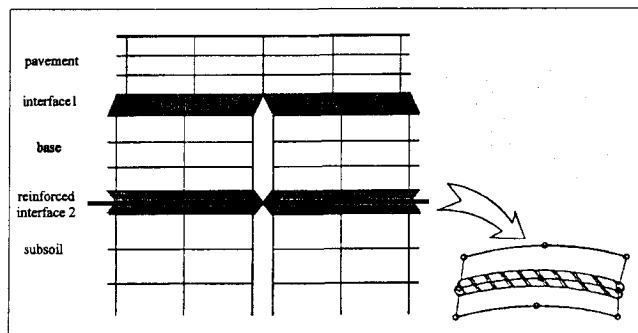
Starting from the initial cracked structural layer configuration as input by user, the following steps are performed by the system:

1. the ordinary finite elements surrounding the crack tip are substituted by singular elements (see Fig.3).
2. an analysis is performed for the specified load combination and material properties.
3. the singular elements surrounding the current crack tip are automatically replaced by ordinary elements and the new crack tip node is identified.
4. the elements on either side of the incremental crack extension path MN, Fig.3, are disconnected and their nodal loads redistributed to the pavement.

The above procedure is repeated until the crack reaches the top of the pavement.

## 6. FEM aspects of simulation of reinforced unbound base layer

Adequately anchored reinforcement can delay the speed of crack propagation within the pavement layer (by reducing stress concentration at the crack tip), decrease the deflection of road surface by allowing the development of a tensile force across the crack faces and, also, by enabling the development of the aggregate interaction mechanism, Fig.2 [4].



A schematic representation of a typical FEM simulation of a cracked reinforced unbound base layer is shown in Fig. 4. Finite elements can be used for modelling the geometry of base and asphalt layers and bar type elements for modelling the reinforcement.

Figure 4 FEM simulation of layer interface regions

For the simulation of bond between the reinforcement and the surrounding materials, the arrangement shown as an insert in Fig.4 can be utilized. In this, a bar type finite element (simulating the reinforcement) is incorporated between two interface elements (simulating bond of the reinforcement with the surrounding material). By varying the transverse stiffness  $D_{tt}$  of the interfaces various types of bond can be specified.

## 7. Numerical determination of bond stiffness

In the FE-program the finite elements arrangement can be utilized for simulation of the reinforcement and its bonding characteristics with the surrounding material.

The axial stiffness  $EA$  of the bar element was computed on the basis of available product data sheet of the high modulus geogrid composite [3]. On the basis of experimental results

of pullout tests, Fig.5, an iterative finite elements procedure was utilized for determination of the shear stiffness  $D_{tt}$  of the interface elements simulating bond.

A finite elements model of the experimental pullout specimen is shown in Fig.6. For a given level of normal stress  $\sigma$  and an assumed value of  $D_{tt}$ , a point load  $F$ , corresponding to the maximum experimentally measured pullout resistance, was applied at the front end of the reinforcement.

The pullout displacement of the reinforcement at the point of load application was recorded and compared with the experimental one. The analysis was repeated for other values of  $D_{tt}$  until the recorded displacement was equal to the measured one.

By repeating this methodology for different values of  $\sigma$ , a relation was obtained between the stiffness of bond  $D_{tt}$  and the magnitude of the applied normal stress  $\sigma$ :

$$D_{tt} = 0.0002 - 4 \times 10^{-6} \sigma + 7.2 \times 10^{-6} \sigma^2 \quad (2)$$

It is this relation that is utilized in the pavement simulation studies of the following section.

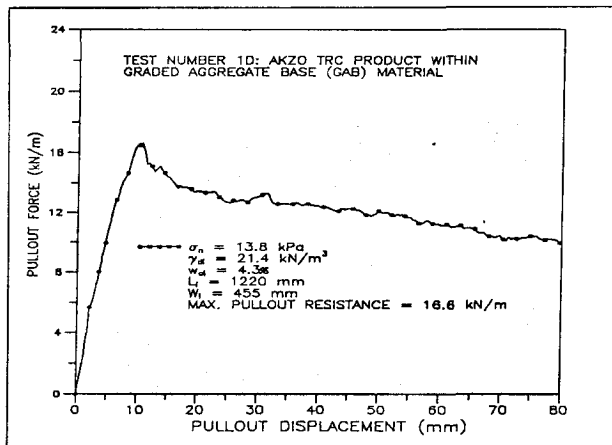


Figure 5 Reinforcement pullout test

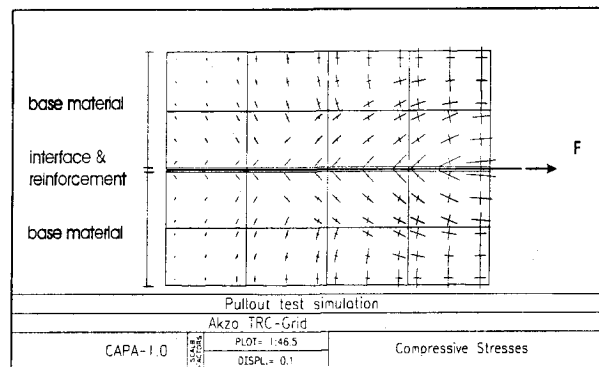


Figure 6 Exaggerated detail of finite element mesh

## 8. Input data FEM simulation of pavements with reinforced base layers

A typical Dutch road profile was selected for numerical simulation. A schematic of the overall pavement geometry and the specified boundary conditions is shown in Fig. 7 and Fig. 8.

As it is typical in most pavement performance prediction studies, the initial crack tip was located at the bottom of the asphalt layer, Fig. 3. In the presentation that follows discussion will be limited to crack propagation due to traffic loads symmetrically placed above the crack plane Fig. 8. A distributed wheel load of 0.707 MPa over a distance of 300 mm was specified in all analyses.

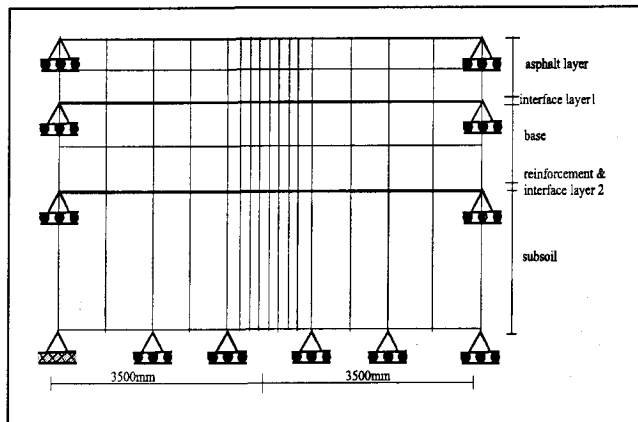


Figure 7 Schematic of pavement mesh characteristics

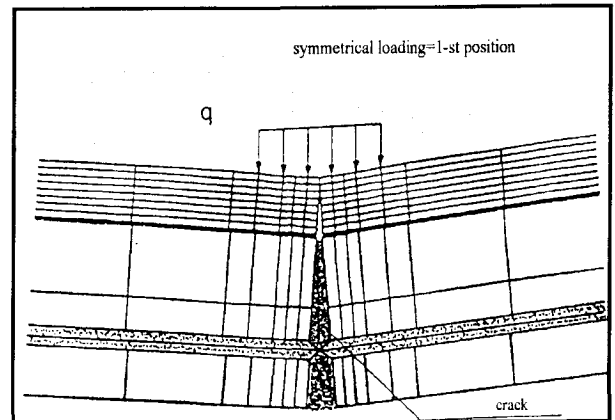


Figure 8 FEM simulation of traffic load directly

The material properties and the thickness of the individual layers are presented in Table 1. Both pavements with unreinforced unbound bases and pavements with reinforced unbound bases were examined. Two levels of reinforcement bond stiffness were examined, Table 2.

Table 1 Material properties and thickness of individual layers

|                  | Thickness<br>[mm] | $E_t$<br>[MPa] | $\nu_t$<br>[--] | $E_n$<br>[MPa] | $\nu_n$<br>[--] | G<br>[MPa] |
|------------------|-------------------|----------------|-----------------|----------------|-----------------|------------|
| asphalt concrete | 160               | 5000           | ---             | 5000           | 0.35            | ---        |
| Base             | CN                | 600~300        | 205             | 410            | 0.35            | 205        |
|                  | CC                | 600~300        | 120.5           | 241.5          | 0.35            | 120.5      |
|                  | CM                | 600~300        | 48.4            | 96.8           | 0.35            | 48.4       |
| Subsoil          | CBR1.5            |                | 0.1             | 22.8           | 0.35            | 11.4       |
|                  | CBR2.5            | Infinite       | 0.1             | 31.6           | 0.35            | 15.8       |
|                  | CBR4.5            |                | 0.1             | 46.1           | 0.35            | 23.0       |

Table 2 Reinforcement bond stiffness

|                   | Thickness<br>[mm] | EA<br>[N/mm] | $D_{tt}$<br>[N/mm]/[mm] <sup>2</sup> | $D_{nn}$<br>[N/mm]/[mm] <sup>2</sup> |
|-------------------|-------------------|--------------|--------------------------------------|--------------------------------------|
| Interface layer 1 | 1                 | ---          | 0.5                                  | 5000                                 |
| Interface layer 2 | 2                 | ---          | 0.1 or 10                            | varies                               |
| Reinforcement     | Type 1            | 8,000        |                                      |                                      |
|                   | Type 2            | 12,000       |                                      |                                      |
|                   | Type 3            | 16,000       |                                      |                                      |

With:

E = isotropic material Young's modulus

$E_t$  = anisotropic material Young's modulus in horizontal direction

$E_n$  = anisotropic material Young's modulus in normal direction

EA = axial stiffness of the reinforcement

$D_{tt}$  = interface element shear stiffness

$D_{nn}$  = interface element normal stiffness

G = anisotropic material shear modulus

$v_t$  = anisotropic material Poisson's ratio in horizontal direction

$v_n$  = anisotropic material Poisson's ratio in normal direction

Type 1, Type 2, Type 3 = aramid geogrid composite with tensile strength of 20, 30, 40 kN/m

CN---crush natural aggregates; CC---crush concrete; CM---crush masonry

Note: The relationship between Young's Modulus and the CBR value of subsoil materials

can be obtained from TRRL equation[5]:  $E = 17.6(CBR)^{0.64}$  (3)

in which: E = Young's modulus [MPa] and CBR = California Bearing Ratio [%]

## 9. Results FEM simulation

### 9.1 Unreinforced unbound base pavements

In order to quantify the effects of substituting natural aggregate materials with recycled ones, parametric analyses were performed of unreinforced pavements consisting of different base materials. A natural aggregate (CN) and two recycled aggregate materials, crushed concrete (CC) and crushed masonry (CM) were examined. A base layer thickness (H) of 45 cm was assumed. As mentioned above, in the following, the discussion will focus on the effects of crack propagation on pavement service life time.

In Fig. 9, a comparison is made of the influence of material type on the service life of the pavement. The term relative life factor (RLF) is utilized. It is defined as:

$$RLF = \frac{N}{N_{ref}} \quad (4)$$

in which  $N_{ref}$  is the number of traffic passes required for the crack at the bottom of the asphalt layer of the pavement with natural aggregate base (CBR=1.5) to propagate to the top and N is the corresponding number for any of the other pavements under comparison.

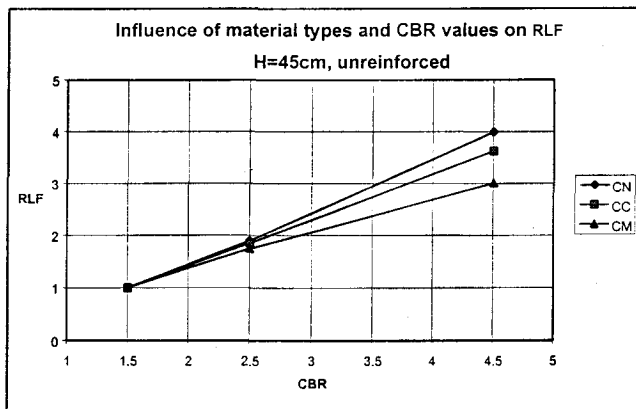


Figure 9 RLF values vs. CBR

When the materials consisting the subsoil of the pavement are not stiff enough to restrain deformations, it is the stiffness characteristics of the material surrounding the crack tip that controls the rate of crack propagation. Hence almost identical RLF are computed for the various pavement types.

As the stiffness of the subsoil increases, the stiffness of the aggregate material, between the subsoil and the asphalt concrete, becomes of greater importance in determining the overall response characteristics of the pavement. For better quality aggregates (CN) the stiffness increases, the deformations decrease and hence a longer pavement service life time is expected, Fig. 9.

In the following section, the contribution of reinforcement in improving the service lifetime of pavements with bases from recycled aggregate materials will be presented.

### 9.2 Reinforced unbound base pavements

Inclusion of reinforcement in the base layer was expected to increase both the stiffness and the force transfer characteristics of the pavement and, as a result, diminish the energy available for crack propagation. In order to verify this postulate, reinforcement was included at the interface between the base and the subsoil of the finite elements mesh of Fig. 7 and the analyses were repeated for various combinations of the input parameters. As indicated in Table 2, two values of bond stiffness and a range of reinforcement stiffness values were utilized.

In Fig. 10, for a different subsoil condition and given unbound CM base thickness, the RLF expresses the improvement of reinforced pavement lifetime over the unreinforced case (H=30cm, CBR=1.5).

For pavements, as the thickness of the base increases, the lever arm of the force couple exerted by the reinforcement increases as well. This additional force/moment carrying mechanism contributes to the structural stiffness of the pavement cross-section, reduces the deflections and hence the energy available for crack propagation, and, it results, eventually, to an overall performance improvement.

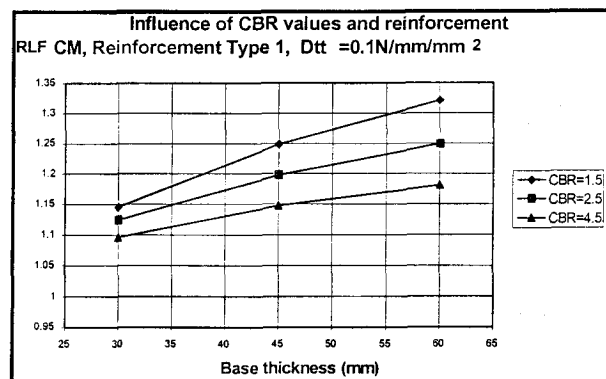
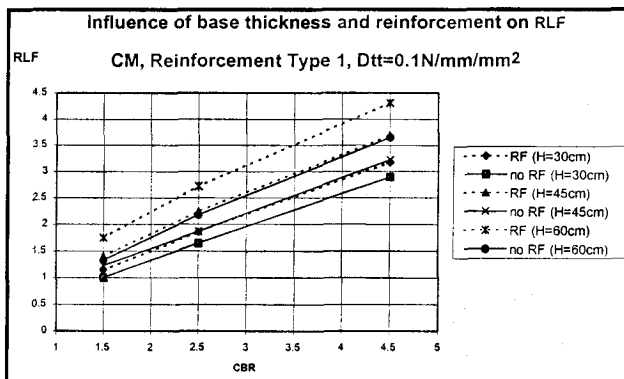


Figure 10 Influence of base thickness and reinforcement Figure 11 Influence of CBR and reinforcement

In Fig. 11 for a given CBR and unbound CM base thickness, the RLF expresses the improvement of reinforced pavement lifetime over that of the corresponding unreinforced. It can be observed that for pavements on soft subsoils, reinforcement makes a significant contribution to the overall pavement stiffness. This increase in stiffness results to an

immediate improvement of RLF. For a given CBR, the effects of increasing the stiffness EA of reinforcement on RLF can be seen in Fig. 12.

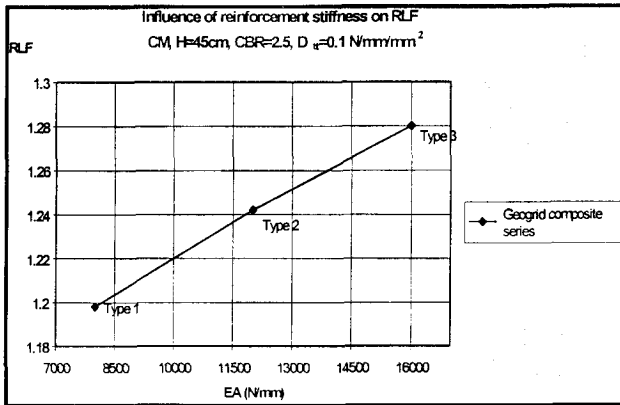


Figure 12 Influence of reinforcement stiffness on RLF

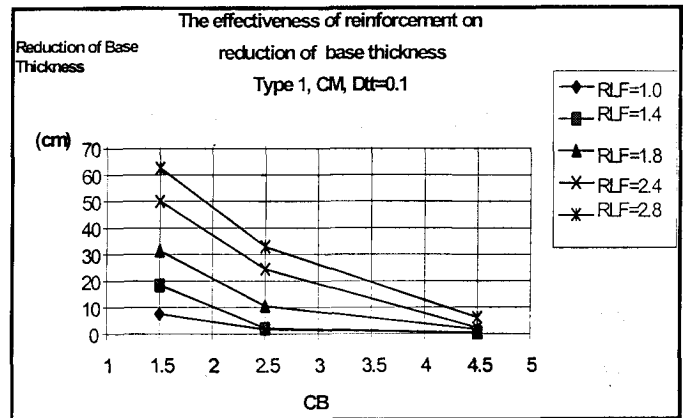


Figure 13 The effectiveness of reinforcement on base thickness

For different subsoil CBR-values, the influence of reinforcement on base thickness is shown in Fig. 13. We first assume the RLF is 1.0 when the pavement base layer constructed from crushed masonry is built on soft subsoil (CBR=1.5) and the thickness of base is 30cm. All the other comparisons are made by modeling the increasing the base thickness of this type of pavement and in the meantime increase the subsoil condition. It is observed that by keeping the service life time of both the unreinforced and reinforced pavement the same, the contribution of reinforcement on the reduction of base thickness is significant especially on soft subsoil condition.

### 9.3 Design charts

Based on the outcome of the FE-analysis several practical design charts can be established. One design chart is presented, the increase of road life due to type 1 reinforcement with CM base, Fig. 14. This chart can be used when the owner of a roadstructure is willing to increase the roadlife by incorporating a geogrid composite in the normal design.  $H_u$  is the unreinforced thickness,  $H_r$  is the thickness of the structure when a geogrid composite is incorporated. Hence,  $H_u$  is equal to  $H_r$ .

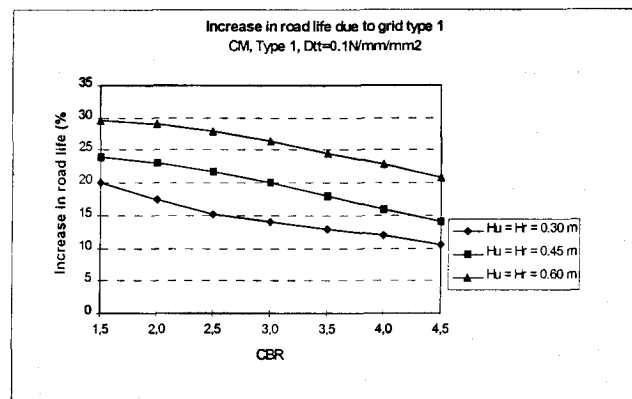


Figure 14 Influence of reinforcement on roadlife

Full scale field tests may be executed to verify the results. However, as many parameters are involved in designing roadstructures with geosynthetics it is hard to develop a proper

testsystem in which all parameters can be kept constant. Therefore, a FE-analysis is a perfect tool to measure the influence of each parameter.

## 10. Conclusion

- In pavements with unbound bases constructed from recycled aggregate materials, the use of adequately anchored multifunctional geogrid composites as reinforcement enhances the tensile force transfer characteristics of the unbound base resulting thus to an overall increase of pavement structural stiffness.
- By compensating for the loss of pavement structural stiffness due to the inferior stiffness properties of the recycled material, multifunctional geogrid composites can prolong the economic life of the construction and hence, render viable the substitution of expensive primary aggregate materials with cheaper secondary ones like crushed concrete and crushed masonry.
- Increasing the stiffness of geogrids and their bonding characteristics with the surrounding materials can effectively reduce, if not annihilate, the energy available for crack extension and hence reduce the speed of crack propagation.
- Out of this FE-analysis design charts can be developed for both the increase of roadlife and the reduction of subbase when a geogrid composite is incorporated in an existing road design.

## 11. References

1. Perkins, S.W. and Ismeik, M. (1997), "A synthesis and evaluation of geosynthetics-reinforced based layers in flexible pavements", Geosynthetics International, Vol. 4 No. 6.
2. Scarpas, A. (1995) "CAPA-2D Finite Elements System-User's Manual", Parts I,II and III, Dept. of Structural Mechanics, Faculty of Civil Engineering, Delft Technical University, Delft, the Netherlands.
3. Product Information Enkagrid TRC, Colbond Geosynthetics, September 1999, the Netherlands
4. Scarpas, A. (1994) "Simulation of Load Transfer Across Joints in RC Pavements", 3-rd International Workshop on the Design and Evaluation of Concrete pavements, Session 3: Materials, Krumbach, Austria.
5. Sweere, G.T.H. "Unbound Granular Base For Roads", Ph.D. Dissertation, Faculty of Civil Engineering, Delft Technical University, Delft, The Netherlands.